https://www.cytojournal.com/

CytoJournal

Editor-in-Chief:
Miaoqing Zhao, PhD., MD (Shandong First Medical University, Jinan, China)
He Wang, MD, PhD (Yale University School of Medicine, New Haven, Connecticut, USA)
Founding Editor & Editor-in-chief Emeritus:
Vinod B. Shidham, MD, FIAC, FRCPath (WSU School of Medicine, Detroit, USA)

OPEN ACCESS

Research Article

FTO-mediated regulation of Kupffer cell polarization and interleukin-6 secretion promotes biliary epithelial cell proliferation in intrahepatic bile duct stones

Lixiang Li, M.S.[1,2,3,4], Hui Peng, M.S.[2,3,4], Ziyi Li, M.S.[2,3,4], Fuhai Zhou, M.S.[2,3,4], Qingsheng Yu, M.S.[2,3,4]

[1]Department of Hepatobiliary Surgery, Lujiang County People's Hospital, [2]Department of General Surgery, The First Affiliated Hospital of Anhui University of Chinese Medicine, [3]Institute of Chinese Medicine Surgery, Anhui Academy of Chinese Medicine, [4]The First Clinical Medical College of Anhui University of Chinese Medicine, Hefei, China.

***Corresponding author:**
Qingsheng Yu,
Department of General Surgery, The First Affiliated Hospital of Anhui University of Chinese Medicine, Hefei, China.

qsy6312@163.com

Received: 20 September 2024
Accepted: 26 November 2024
Published: 31 December 2024

DOI
10.25259/Cytojournal_193_2024

Quick Response Code:

ABSTRACT

Objective: Intrahepatic cholangiolithiasis (Intrahepatic bile duct stones, IBDSs) is a common hepatobiliary disease characterized by bile duct obstruction and inflammation, often leading to severe complications such as cholangitis, cirrhosis, and cholangiocarcinoma. This study investigates the role of fat mass and obesity-associated (FTO) protein, an RNA demethylase, in regulating Kupffer cell (KC) polarization, interleukin (IL)-6 secretion, and subsequent human intrahepatic biliary epithelial cell (HiBEC) proliferation in IBDS.

Material and Methods: Liver tissues from patients with IBDS were analyzed for FTO expression, KC M2 polarization, and IL-6 levels. *In vitro* experiments with FTO silencing in KCs were conducted to examine the effects on M2 polarization, IL-6 production, and HiBEC proliferation. Mechanistic analysis focused on the c-Jun N-terminal kinase (JNK)/p38 and phosphoinositide 3-kinase (PI3K)/protein kinase B (AKT) pathways.

Results: The patients with IBDS showed significantly higher KC M2 polarization, elevated FTO expression, and increased IL-6 levels relative to the controls. Without FTO silencing, IL-6 secretion and HiBEC proliferation remained at high baseline levels. However, FTO silencing reduced M2 polarization, IL-6 secretion, and HiBEC proliferation through the JNK/p38 pathway. Activating the PI3K/AKT pathway partially reversed these inhibitory effects.

Conclusion: FTO plays a critical role in IBDS by promoting the M2 polarization of KCs, which leads to increased IL-6 secretion and induced pathological HiBEC proliferation. Targeting FTO may represent a novel therapeutic strategy for managing IBDS and preventing disease progression.

Keywords: Intrahepatic, Cholangiolithiasis, Kupffer cells, Interleukin-6, Cholangiocytes

INTRODUCTION

Intrahepatic bile duct stones (IBDS) is a prevalent and complex hepatobiliary disease characterized by the formation of stones within the bile ducts, leading to biliary obstruction, cholangitis, and impaired liver function and severely affecting the quality of life and prognosis.[1] First described in Hong Kong in 1930,[2] IBDS has varying prevalence across different regions and populations. While IBDS is relatively rare in Western countries, its incidence is notable in East Asian countries, particularly China, Japan, and South Korea. This disparity is possibly influenced by dietary habits, genetic factors, and the high prevalence of biliary infections in these regions.[3]

Epidemiological studies have shown that the prevalence of IBDS in China is approximately 2–0.5%, with the majority of cases occurring in the middle-aged and elderly population.[4] Age-related decline in biliary system function, changes in bile composition, and weakened immune response may further increase the risk of stone formation. Despite advancements in imaging techniques and minimally invasive treatments, high recurrence rates and complications continue to pose challenges in the clinical management of this disease.[5]

The pathogenesis of IBDS remains complex and poorly understood.[6] Contributing factors may include bile stasis, biliary infection, anatomical abnormalities of the bile ducts, altered bile metabolism, malnutrition, and dietary influences.[7,8] Patients with anatomical or functional changes in the biliary system are at a high risk of developing liver stones. Congenital and/or acquired intrahepatic bile duct abnormalities, such as Caroli disease, primary sclerosing cholangitis, and anastomotic strictures, are major risk factors. These strictures lead to nonlinear bile flow, which promotes crystal aggregation and stone formation within the bile ducts.[9] Chronic inflammation induces bile duct deformities, resulting in strictures and/or dilation. These changes alter bile rheology due to irregularities in the ductal surface. Furthermore, many proliferating glandular cells exhibit mucin-producing activity. Excess mucin secreted into the bile ducts may create a microenvironment that is conducive to stone formation by adsorbing calcium salts and lipids.[10]

The proliferation of biliary epithelial cells plays a pivotal role in the pathogenesis of biliary diseases, particularly in bile duct strictures. Chronic inflammation or bile duct injury typically triggers excessive human intrahepatic biliary epithelial cell (HiBEC) proliferation, progressively narrowing the bile ducts and leading to biliary obstruction and impaired bile flow.[11] This pathological process is accompanied by abnormal extracellular matrix deposition and fibrotic tissue formation, further exacerbating the stricture. Understanding HiBEC proliferation and its relationship with bile duct strictures is essential for identifying potential therapeutic targets to prevent or treat biliary strictures.

Recent research has highlighted the role of the liver's immune microenvironment and Kupffer cells (KCs) in the development of intrahepatic cholangiolithiasis. KCs, the liver's resident macrophages, play critical roles in immune surveillance and inflammatory responses.[12] The polarization state of KCs significantly effects disease progression and prognosis in liver diseases.[13-15] During liver injury, KCs become activated and are involved in inflammation and tissue repair.[16] However, the role of KC polarization in IBDS remains unclear.

Interleukin (IL)-6, a key pro-inflammatory cytokine, plays important roles in various liver diseases.[17] It promotes inflammatory responses and supports HiBEC proliferation and survival through autocrine and paracrine mechanisms.[18] The IL-6 secreted by KCs and other liver immune cells can drive HiBEC proliferation, contributing to the progression of biliary strictures.[19] KC polarization regulates IL-6 secretion following liver injury. Wang *et al*.[20] demonstrated that M2-polarized KCs promote IL-6 secretion, which, in turn, induces hepatocyte senescence. IL-6 is also involved in the crosstalk between HiBECs and immune cells. IL-6 signaling activates the signal transducer and activator of transcription 3 (STAT3) pathway to inhibit bacterial infections, promote epithelial cell proliferation, and prevent epithelial apoptosis, thus exerting an anti-inflammatory effect.[21] The primary objectives of the present study are to investigate the role of fat mass and obesity-associated (FTO) in regulating KC polarization and IL-6 secretion and to further explore how these immune-related changes influence HiBEC proliferation and migration in IBDS. We hypothesize that increased FTO expression promotes the M2 polarization of KCs to increase IL-6 secretion, which, in turn, enhances HiBEC proliferation and migration. This phenomenon contributes to bile duct narrowing and the development of intrahepatic cholangiolithiasis.

This study is the first to elucidate the mechanism by which FTO regulates KC polarization and IL-6 secretion and the subsequent effects on HiBEC proliferation and migration in patients with intrahepatic cholangiolithiasis. Our results show a significant increase in M2-polarized KCs, accompanied by elevated FTO expression and IL-6 levels in patients with IBDS. *In vitro* experiments further confirmed that silencing FTO inhibits KC M2 polarization and reduces IL-6 secretion, thereby suppressing HiBEC proliferation and migration. We also found that FTO modulates KC polarization through the c-Jun N-terminal kinase (JNK)/p38 signaling pathway, and activation of the phosphoinositide 3-kinase (PI3K)/protein kinase B (AKT) pathway can counteract the inhibitory effects of FTO knockdown on HiBEC proliferation. These findings provide new insights into the pathogenesis of IBDS and suggesting that FTO, through its regulation of the immune microenvironment and KC polarization, plays a key role in bile duct strictures and stone formation. This study lays the groundwork for future research exploring the role of FTO in other biliary diseases.

MATERIAL AND METHODS

Patient sample selection and ethical approval

The research protocol was in accordance with the principles outlined in the Declaration of Helsinki and received approval from the Medical Ethics Committee of Lujiang People's Hospital (Approval number: LYWZLL202304). Written informed consent was obtained from all the participants before the collection and analysis of samples.

Between January 2022 and December 2023, liver tissue samples were acquired from 30 patients diagnosed with IBDS

who had surgical resections at Lujiang People's Hospital. The inclusion criteria were as follows: (1) confirmed diagnosis of IBDS through imaging (such as CT or MRI), (2) presence of bile duct strictures related to stone formation, and (3) no past history of hepatocellular carcinoma or other biliary malignancies. Control liver tissue samples were taken from 10 patients who had surgeries for benign liver lesions not related to IBDS (e.g., hemangioma) and no history of biliary or inflammatory liver disease.

Flow cytometry analysis and immunohistochemistry (IHC) were conducted on the samples to assess KC polarization and FTO expression in human liver tissues. No *in vitro* studies were performed on the KCs derived from the patients. Short tandem repeat profiling was performed on the patient liver cells to confirm their origin and authenticity. The analysis followed standard protocols, ensuring reliable identification of the cell source.

Cell culture and transfection

Male C57BL/6 mice (6–8 weeks old, 20–25g) were purchased from Beijing Vital River Laboratory Animal Technology, China, and housed under specific pathogen-free (SPF) conditions. Mice were maintained in a controlled environment (22±2°C, 55±5% humidity, 12-hour light/dark cycle) with ad libitum access to sterilized food and water. At the end of the study, mice were euthanized by intraperitoneal injection of an overdose of sodium pentobarbital (200 mg/kg, Sigma-Aldrich, USA), ensuring painless sacrifice. All animal experiments were conducted following ethical guidelines and were approved by the Animal Ethics Committee of Lujiang People's Hospital (number LYWZLL202304). The study adhered to the principles outlined in the Guide for the Care and Use of Laboratory Animals, ensuring humane treatment of the animals throughout the experimental procedures. Liver tissue was enzymatically digested with type IV collagenase (Catalog #C5138, Sigma-Aldrich, USA) and then separated through discontinuous density gradient centrifugation to isolate the KCs. The purified KCs were cultured in RPMI 1640 medium, supplemented with 10% fetal bovine serum (FBS) (Catalog #16000044, Gibco, USA) and 1% penicillin–streptomycin (Catalog #15140122, Gibco, USA). The coculturing of KCs with HiBECs was performed in Transwell chambers (0.4 μm PET, Millipore), where treated KCs (either with FTO knockdown or overexpression) were placed in the lower chamber and HiBECs were introduced into the upper chamber at a 5:1 ratio. The culture medium used was RPMI 1640 containing 10% FBS and 1% antibiotics. This coculture setup was maintained for 24–48 h to assess the impact of KCs on biliary epithelial cells.

The small interfering RNA (siRNA) targeting FTO was synthesized by Genscript Biotech Corporation with the following sequences: small interfering RNA targeting FTO (si-FTO) sense: 5'-GCUUCUCUCUUCAUCAAAATT-3', antisense: 5'-UUUUGAUGAAGAGAGAAGCTT-3', and for the negative control siRNA (si-NC): sense: 5'-UUC UCCGAACGUGUCACGUTT-3', antisense: 5'-ACG UGACACGUUCGGAGAATT-3'. The p38 signaling pathway activator, Trifluoroacetic acid (TFA), was acquired from MedChemExpress (Catalog #HY-13837, MedChemExpress, USA). Once the cells reached 80% confluence, transfection was performed using Lipofectamine 3000 (Catalog #L3000015, Invitrogen, USA) as per the manufacturer's instructions. After allowing the siRNA-lipid complexes to incubate for 15 min at room temperature, they were introduced to the KCs. Gene expression was assessed 48 h post-transfection, and the KCs were treated with TFA for 24 h before the transfection to activate the JNK signaling pathway. For all the cell samples derived from patients and mice, mycoplasma testing was performed to ensure the absence of contamination.

Quantitative polymerase chain reaction (qPCR)

RNA was extracted from the cells and tissues using TRIzol reagent (Invitrogen, Carlsbad, CA, USA, Cat# 15596018) as per the manufacturer's instructions. The isolated RNA was then converted into complementary DNA (cDNA) through reverse transcription by utilizing the RevertAid First Strand cDNA Synthesis Kit (Thermo Fisher Scientific, Cleveland, OH, USA, Cat# K1622), following the recommended procedure. Real-time qPCR was carried out using PowerUp SYBR Green Master Mix (Applied Biosystems, Foster City, CA, USA, Cat# A25742) on the QuantStudio 3 Real-Time polymerase chain reaction System (Model QuantStudio 3, Applied Biosystems, USA).

The primer sequences for qPCR are provided in Table 1, with glyceraldehyde-3-phosphate dehydrogenase (GAPDH)

Table 1: Primer sequences.

Name	Primers for PCR (5′-3′)
Arg-1	
Forward	ACTTAAAGAACAAGAGTGTGATGTG
Reverse	CATGGCCAGAGATGCTTCCA
CD206	
Forward	ACCTGCGACAGTAAACGAGG
Reverse	TGTCTCCGCTTCATGCCATT
GAPDH	
Forward	TCCCATCACCATCTTCCAGG
Reverse	GATGACCCTTTTGGCTCCC
CD86	
Forward	GCTTGCAACAGATCGTTGCAGG
Reverse	TGGTTGGTGTCCTTGGATCGAG

PCR: Polymerase chain reaction, GAPDH: Glyceraldehyde-3-phosphate dehydrogenase, A: Adenine, C: Cytosine, G: Guanine, T: Thymine

serving as the internal control for gene expression normalization. The relative expression of the target genes was determined using the $2^{-\Delta\Delta CT}$ method. All experiments were repeated in triplicate to ensure accuracy, and data analysis was performed with QuantStudio software (Applied Biosystems1.5.2, Thermo Fisher Scientific, USA).

Enzyme-linked immunosorbent assay (ELISA)

The cytokine and protein levels in the cell culture supernatants and tissue lysates were quantified using ELISA kits for IL-6 (Catalog #D6050, R&D Systems, USA) and tumor necrosis factor-alpha (Catalog #BMS223HS, Thermo Fisher Scientific, USA). In brief, 96-well plates were coated with 100 μL of capture antibody in coating buffer and left to incubate overnight at 4°C. The plates were then washed with PBST (0.05% Tween-20 in phosphate-buffered saline [PBS]) and blocked with 1% bovine serum albumin (BSA) for 1 h at room temperature. After an additional wash, 100 μL of diluted standards or samples was added to each well and incubated for 2 h at room temperature. The samples were applied with 100 μL of biotinylated detection antibody and incubated for 1 h, followed by a 30-min incubation with 100 μL of streptavidin-Horseradish peroxidase (HRP) conjugate in the dark. After another wash, 100 μL of TMB substrate was added to develop the color, and the reaction was stopped by adding 50 μL of 2N H_2SO_4 when the desired color intensity was reached. Absorbance was measured at 450 nm using a BioTek microplate reader (model EL ×800), and protein concentrations were calculated based on a standard curve.

IHC

IHC was conducted on the liver tissue sections to investigate the target protein expression. The liver samples were fixed in 10% neutral-buffered formalin for 24 h, embedded in paraffin, and sectioned into 4 μm slices. The sections were then deparaffinized in xylene, rehydrated through graded ethanol concentrations, and subjected to antigen retrieval in citrate buffer (pH 6.0) or EDTA buffer (pH 9.0) at 95°C–100°C for 15–20 min. After cooling, 3% hydrogen peroxide in methanol was used to block endogenous peroxidase, followed by a blocking step with 5% BSA or normal serum. Primary antibodies against FTO (Catalog #ab92821, Abcam, UK, 1:1000) and CD68 (Catalog #76437, Cell Signaling Technology, USA, 1:100) were applied, and the sections were incubated overnight at 4°C. The following day, a biotinylated secondary antibody and an avidin-biotin complex (ABC kit, Vector Laboratories, Catalog # PK-6100) were used. Diaminobenzidine (Dako, Catalog # K3468) was added as a chromogen, and hematoxylin was used for counterstaining. The sections were subsequently dehydrated, cleared in xylene, and mounted for microscopy. Negative controls were prepared without the primary antibody, and positive controls were incorporated with tissues known for expressing the target proteins.

Western blot

For the Western blot analysis, proteins were extracted from the cell and tissue lysates using RIPA lysis buffer (Beyotime, P0013B) containing protease and phosphatase inhibitors. Protein concentrations were determined using a BCA protein assay kit (Thermo Fisher Scientific, 23225). Equal protein amounts (30 μg per sample) were loaded onto 10% SDS-PAGE gels for separation, followed by transfer onto polyvinylidene difluoride membranes (Millipore, IPVH00010). The membranes were blocked with 5% nonfat milk in Tris-buffered saline with 0.1% Tween-20 at room temperature for 1 h and then incubated overnight at 4°C with primary antibodies, including anti-FTO, anti-JNK (Catalog #9252, Cell Signaling Technology, USA, 1:1000), anti-phospho-JNK (p-JNK) (Catalog #9255, Cell Signaling Technology, USA, 1:1000), anti-p38 (Catalog #8690, Cell Signaling Technology, USA, 1:1000), anti-phospho-p38 (p-p38) (Catalog #4511, Cell Signaling Technology, USA, 1:1000), and anti-GAPDH (Catalog #60004-1-Ig, Proteintech, USA, 1:5000) as a loading control. After washing, the membranes were treated with HRP-conjugated anti-rabbit Immunoglobulin G (IgG) (Catalog #7074, Cell Signaling Technology, USA, 1:5000) or HRP-conjugated anti-mouse IgG (Catalog #7076, Cell Signaling Technology, USA, 1:5000) for 1 h at room temperature. Protein bands were visualized using enhanced chemiluminescence reagents (Thermo Fisher Scientific, 32106) and captured with the ChemiDoc™ XRS + system (Bio-Rad, 1708265). Band intensities were analyzed with ImageJ software (1.5.3, National Institutes of Health, USA).

Cell viability assay

Cell viability was evaluated using the 3-(4,5-dimethylthiazol-2-yl)-2,5-diphenyltetrazolium bromide (MTT) assay (Sigma-Aldrich, M2128). The cells were seeded in 96-well plates (Corning, 3590) at a density of 5×10^3 cells per well in 100 μL of complete medium and incubated overnight to allow attachment. After treatment under different experimental conditions, 10 μL of 5 mg/mL MTT solution was added to each well, and the plates were incubated at 37°C with 5% Carbon dioxide (CO_2) for 4 h. The medium was then carefully removed, and 150 μL of dimethyl sulfoxide (Sigma-Aldrich, D2650) was added to dissolve the formazan crystals. The plates were gently shaken for 10 min to ensure full dissolution. Absorbance was recorded at 570 nm using a microplate reader (Model EL ×800, BioTek, USA). Cell viability was expressed as a percentage relative to the untreated control. Each experiment was repeated in triplicate, and the results were presented as mean ± standard deviation (SD).

5-ethynyl-2′-deoxyuridine (EdU) incorporation method

The EdU incorporation assay (Click-iT™ EdU Imaging Kit, Thermo Fisher Scientific, C10337) was used to measure cell proliferation. The cells were seeded into 24-well plates (Corning, 3524) at 2×10^4 cells per well and allowed to attach overnight in complete growth medium. EdU was added at a concentration of 10 μM, and the cells were incubated for 2 h at 37°C with 5% CO_2 to permit EdU incorporation during DNA replication. After incubation, the cells were fixed in 4% paraformaldehyde (Catalog #158127, Sigma-Aldrich, USA) for 15 min, followed by permeabilization with 0.5% Triton X-100 (Catalog #T8787, Sigma-Aldrich, USA) for 20 min. The Click-iT™ reaction cocktail was then applied to label incorporated EdU as per the manufacturer's protocol. Nuclei were stained with 4′,6-Diamidino-2-phenylindole (DAPI) (Catalog #D1306, Thermo Fisher Scientific, USA) for 10 min to visualize cell nuclei. Images were captured under a fluorescence microscope (Model DMi8, Leica, Germany), and the percentage of cells with EdU incorporation was calculated relative to the DAPI-stained nuclei. Each test was conducted in triplicate, and the data were reported as mean ± SD.

Wound healing assay

The cells were seeded in six-well plates (Corning, 3516) at a density of 5×10^5 cells per well and cultured until they reached 90–100% confluence. A sterile 200 μL pipette tip was used to create a scratch across the center of each well to mimic a wound. After the scratch was created, the cells were rinsed twice with PBS (Thermo Fisher Scientific, 10010023) to remove any debris, and fresh serum-free medium was added to restrict cell proliferation. The cells were then incubated at 37°C in a 5% CO_2 atmosphere, and phase-contrast images were taken at 0 and 24 h (Leica, DMi8) to monitor wound healing. Wound width was measured at each time point using ImageJ software, and the percentage of closure was determined by comparing the initial wound area (0 h) to the area at 24 h. All the experiments were conducted in triplicate, and the data were reported as mean ± SD.

Statistical analysis

All experiments were performed in triplicate, and the data were presented as mean ± SD. Statistical analysis was conducted using GraphPad Prism software (GraphPad Software, San Diego, CA, USA, Version X). Significant differences between groups were evaluated using one-way ANOVA followed by Tukey's *post hoc* test or two-way ANOVA where appropriate. For comparisons between two groups, an unpaired Student's *t*-test was used. $P < 0.05$ was considered statistically significant. The specific statistical tests used are indicated in the figure legends.

RESULTS

Significantly increased FTO expression and elevated IL-6 levels in the M2-polarized KCs of patients with IBDS

To investigate changes in immune cell polarization, we collected liver tissues surgically resected from patients with IBDS. Compared with that in the control group, the proportion of M2-polarized KCs in the liver tissues of the patients with IBDS was significantly higher [Figure 1a]. Using immunofluorescence to detect the expression of established hepatic M2 macrophage markers CD206 and CD163, we observed a significant increase in fluorescence intensity for CD206 and CD163 in the tissues of the patients with IBDS [Figure 1b]. Meanwhile, IL-6 expression was markedly increased in the IBDS group compared with the baseline levels in the control group [Figure 1c]. These results suggest that KC polarization is markedly altered in patients with IBDS. To further explore the relationship between FTO and KC polarization in IBDS, we examined FTO expression in the KCs of patients with IBDS. Our findings indicate that FTO expression was significantly increased in the KCs of the patient group [Figure 1d].

FTO silencing inhibits M2 polarization in KCs

We transfected primary isolated mouse KCs with si-FTO or si-NC to study the effect of FTO on KC polarization. Gene expression was analyzed 48 h after transfection. The transfection of si-FTO significantly reduced FTO abundance compared with that in the control (si-NC group), confirming the successful knockdown of FTO in the KCs [Figure 2a and b]. Following si-FTO transfection, the levels of M2 polarization markers Arg-1, CD163, and CD206 were decreased in the KCs [Figure 2c]. These results suggest that the downregulation of FTO inhibits M2 polarization in KCs.

FTO silencing inhibits the promotive effects of M2-polarized KCs on the proliferation and migration of HiBECs

Next, we investigated the effect of FTO silencing in KCs on HiBECs. In this experiment, we first induced M2 polarization in KCs and then treated HiBECs with M2-KCs, si-FTO/M2-KCs, or si-NC/M2-KCs. Treatment with M2-KCs promoted HiBEC proliferation, and treatment with si-FTO/M2-KCs reduced HiBEC proliferation [Figure 3a and b]. M2-KCs enhanced HiBEC migration [Figure 3c] and IL-6 secretion [Figure 3d], but this effect was attenuated after si-FTO transfection. These findings suggest that silencing FTO reduces the effects of M2-polarized KCs on HiBEC proliferation and migration and decreases the IL-6 secretion by M2-polarized KCs.

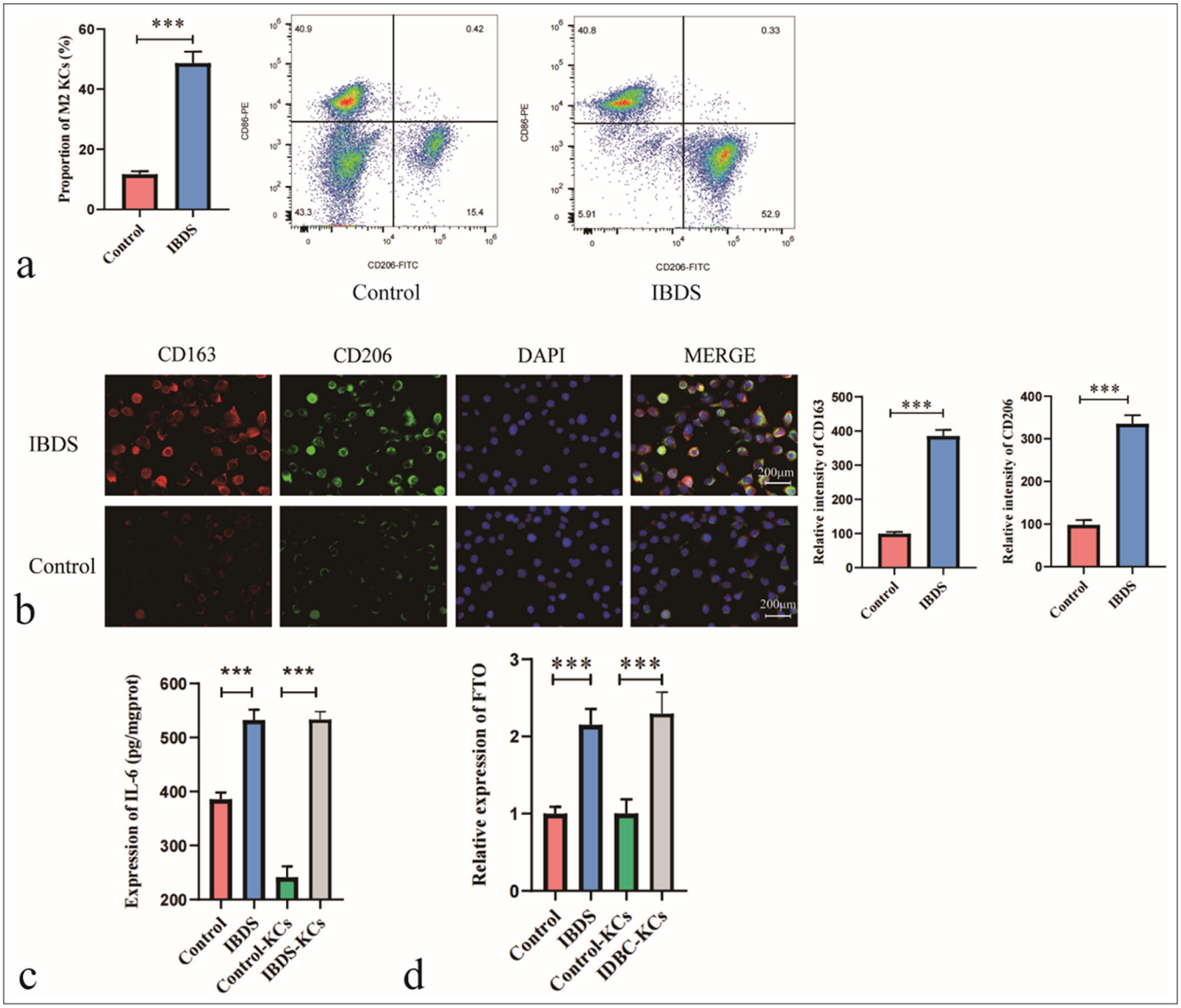

Figure 1: Increased proportion of M2-polarized Kupffer cells (KC) and elevated fat mass and obesity-associated (FTO) expression in patients with intrahepatic bile duct stone (IBDS). (a) Flow cytometry analysis of the proportion of M2-polarized KC in patients with IBDS relative to that in the control group. (b) Immunofluorescence analysis of M2-polarized KC markers CD163 and CD206. (c) Enzyme-linked immunosorbent assay analysis of IL-6 levels in KC. (d) Quantitative polymerase chain reaction analysis of FTO expression levels in KC. ***$P < 0.001$. DAPI: 4',6-Diamidino-2-phenylindole.

FTO knockdown inhibits M2 polarization by suppressing the JNK/p38 signaling pathway

We explored the signaling pathways involved in FTO-induced KC polarization. After pretreatment with TFA, si-FTO or si-NC was transfected into KCs. Key molecules in the signaling pathway and the polarization markers were analyzed 48 h later. The ratios of p-JNK/JNK and p-p38/p38 were reduced following si-FTO transfection [Figure 4a]. TFA treatment attenuated the inhibitory effects of si-FTO transfection on M2 polarization in KCs [Figure 4a]. In addition, TFA treatment blocked the effects of FTO knockdown on the levels of M2 polarization markers Arg-1, CD163, and CD206 in KCs [Figure 4b]. Therefore, we conclude that FTO silencing inhibits M2 polarization in KCs by suppressing the JNK/p38 signaling pathway.

Activation of the PI3K/AKT signaling pathway blocks the FTO-mediated effects on cholangiocyte proliferation

We conducted a rescue experiment to determine whether FTO regulates the effects of M2-polarized KCs on HiBECs through the JNK/p38 signaling pathway. HiBECs were treated with si-NC/M2-KCs, si-FTO/M2-KCs, or TFA + si-FTO/M2-KCs. Treatment with si-FTO/M2-KCs reduced HiBEC proliferation [Figure 5a and b] and migration [Figure 5c], and cotreatment

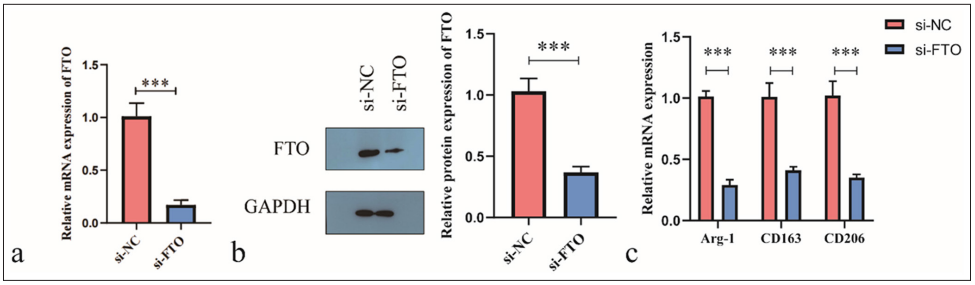

Figure 2: Silencing of fat mass and obesity-associated (FTO) inhibits the M2 polarization of Kupffer cells. (a and b) FTO abundance was evaluated using real-time quantitative polymerase chain reaction (RT-qPCR) and Western blot. (c) RT-qPCR was used to assess the levels of CD163, Arg-1, and CD206. $^{**}P < 0.01$, $^{***}P < 0.001$. si-NC: Negative control si-RNA.

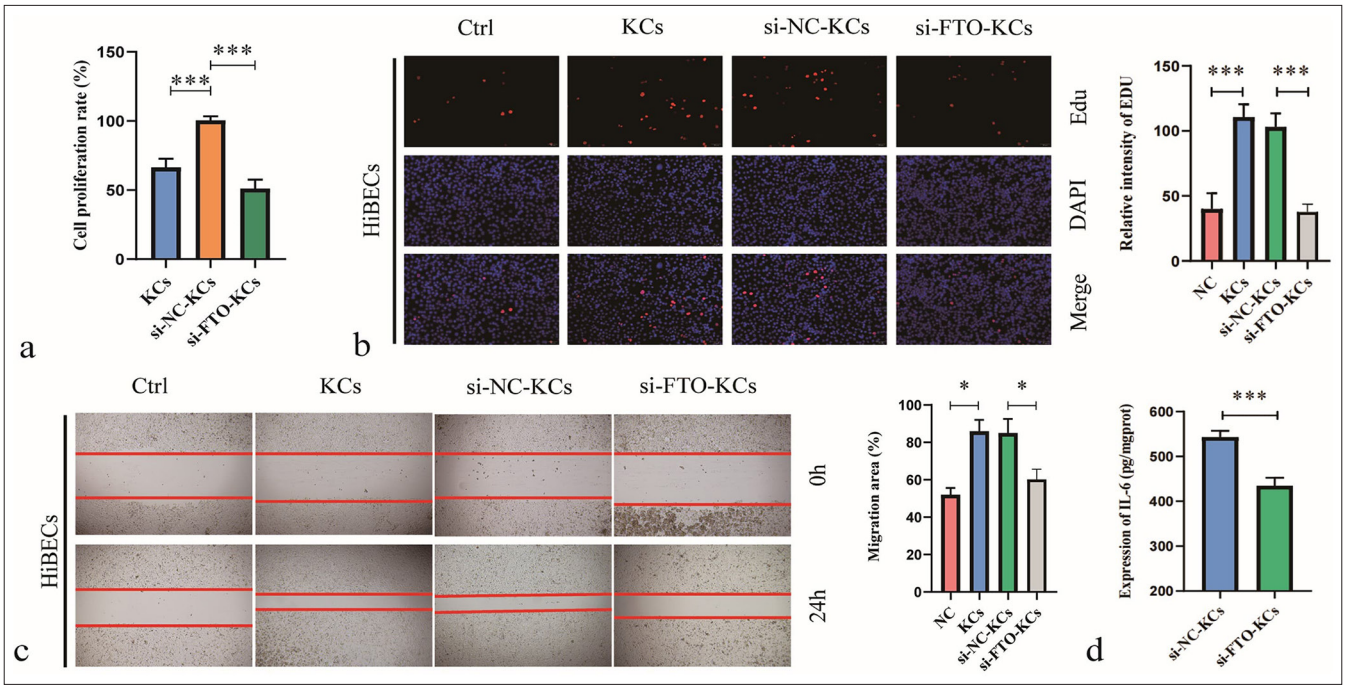

Figure 3: Silencing fat mass and obesity-associated (FTO) inhibits the effects of M2-polarized Kupffer cells (KC) on human intrahepatic biliary epithelial cells. (a) Cell counting kit-8 assay was used to detect cell viability relative to that of the NC group. (b) Cell proliferation was analyzed by 5-ethynyl-2′-deoxyuridine assay. (c) Cell migration was evaluated by wound healing assay. (d) interleukin-6 production was measured by Enzyme-linked immunosorbent assay. $^{*}P < 0.05$, $^{**}P < 0.01$, $^{***}P < 0.001$. NC: negative control.

with TFA restored HiBEC proliferation. Therefore, we confirmed that the activation of the PI3K/AKT signaling pathway attenuates the inhibitory effects of FTO knockdown on M2-polarized KC-induced HiBEC development.

DISCUSSION

IBDS is a common biliary disease characterized by stone formation within the bile ducts and leads to ductal narrowing, obstruction, and bile stasis, which may eventually cause cholangitis, cirrhosis, or even cholangiocarcinoma.[22] Although the exact pathogenesis is not fully understood, recent studies suggest that chronic inflammation, bile stasis, and abnormal proliferation of biliary epithelial cells play critical roles in this illness.[23,24]

This study is the first to report a significant increase in M2-polarized KCs and an elevated IL-6 expression in patients with IBDS compared with those in the control group. M2-polarized KCs play a key role in chronic inflammation and fibrosis, particularly in liver diseases. Licá *et al*.[25] demonstrated that M2-polarized KCs promote tissue repair and fibrosis by secreting pro-inflammatory cytokines and growth factors. Our *in vitro* experiments showed that FTO knockdown in KCs inhibited M2 polarization, reduced IL-6 secretion, and suppressed

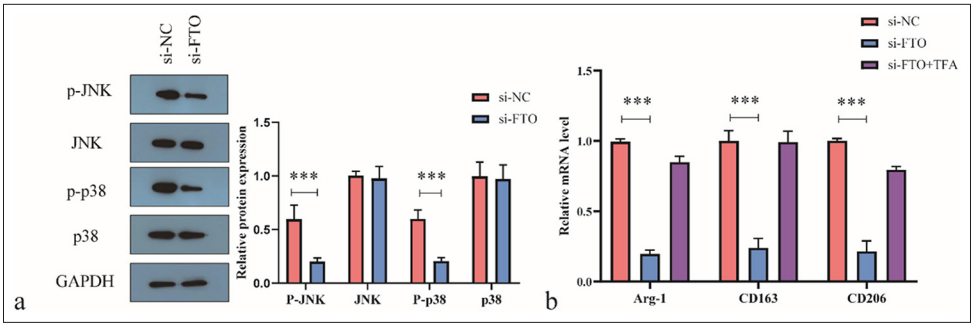

Figure 4: Fat mass and obesity-associated (FTO) silencing reduces M2 polarization of macrophages by inhibiting the c-Jun N-terminal kinase (JNK)/p38 signaling pathway. (a) Western blot analysis of JNK/p38 signaling pathway activity. (b) Real-time quantitative polymerase chain reaction analysis of Arg-1, CD163, and CD206 levels. ***P < 0.001. si-NC: negative control si-RNA, GAPDH: Glyceraldehyde-3-phosphate dehydrogenase, TFA: Trifluoroacetic acid.

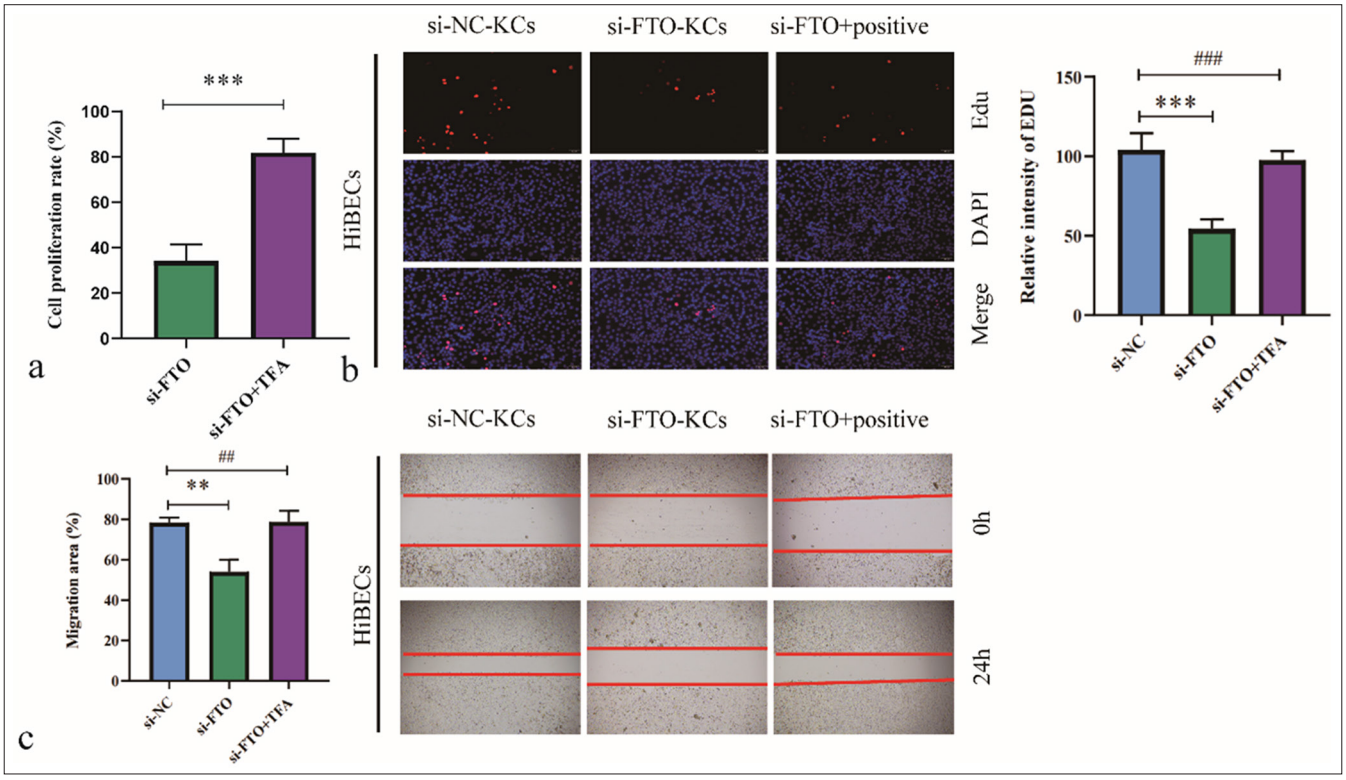

Figure 5: Activation of the c-Jun N-terminal kinase/p38 signaling pathway blocks the effects of fat mass and obesity-associated (FTO) silencing on M2-polarized Kupffer cell (KC)-mediated human intrahepatic biliary epithelial cell proliferation and migration. (a) Cell viability was assessed by cell counting kit-8 assay. (b) Cell proliferation was analyzed by 5-ethynyl-2'-deoxyuridine assay. (c) Cell migration was evaluated by wound healing assay. **P < 0.01, ***P < 0.001. si-NC: negative control si-RNA, TFA: Trifluoroacetic acid. ##/###: No significant difference.

biliary epithelial cell proliferation and migration, offering insights into IBDS progression mechanisms. Our findings indicate that elevated IL-6 levels are associated with IBDS progression, suggesting that FTO may play a regulatory role in the inflammatory cascade. Thus, targeting FTO could provide a therapeutic approach for modulating IL-6 secretion and KC polarization.

Our study is the first to identify the critical role of FTO in IBDS development. Analysis of samples from patients with IBDS revealed significantly increased FTO expression in KCs. This finding aligns with a previous research implicating FTO in chronic inflammation and metabolic diseases.[26] KCs, the resident macrophages of the liver, play a crucial role in immune regulation and tissue repair.[27] FTO overexpression in

KCs promotes M2 polarization and IL-6 secretion, which, in turn, induces the proliferation of biliary epithelial cells. These processes collectively contribute to bile duct narrowing and the formation of intrahepatic cholangiolithiasis. Our findings expand existing knowledge by demonstrating that FTO upregulation promotes M2 polarization and directly influences the pathological proliferation of biliary epithelial cells.

Excessive IL-6 secretion in biliary epithelial cells may activate the STAT3 signaling pathway and thus promote pathological cell proliferation, which contributes to bile duct narrowing and stone formation. Chen *et al*.[28] reported that IL-6 promotes cholangiocarcinoma development through the STAT3 pathway. Our study demonstrated that IL-6 levels are significantly elevated in patients with IBDS and positively correlated with FTO expression, providing new evidence for IL-6 as a potential therapeutic target.

Our results suggest that the high FTO expression in KCs could serve as a potential biomarker for IBDS. This observation is consistent with the findings of Zahr *et al*.,[27] who showed that FTO upregulation is closely associated with liver inflammation and fibrosis and that FTO inhibition can alleviate these pathological conditions. The relationship between FTO and IL-6, particularly in liver diseases, remains underexplored. IL-6 is a key cytokine involved in inflammation and cell proliferation. In our study, we observed that elevated IL-6 levels are correlated with increased FTO expression in patients with IBDS. This result suggests that FTO may regulate IL-6 production at the transcriptional or post-transcriptional level, potentially through m6A RNA modification. This novel finding differentiates our research from earlier studies and positions FTO as a key regulator of immune cell behavior and epithelial cell proliferation in the liver.

Although our study focused on the JNK/p38 signaling pathway, FTO likely influences IL-6 secretion through other potential mechanisms. As an RNA demethylase, FTO may affect the mRNA stability of IL-6 or other key regulatory factors involved in the inflammatory response.[29] A recent work showed that FTO-mediated m6A demethylation may stabilize inflammatory mRNAs and increase their expression, suggesting that FTO could regulate IL-6 mRNA stability via m6A modification.[29] The PI3K/AKT pathway may also be involved, as FTO interacts with this pathway in metabolic regulation and PI3K/AKT activation promotes IL-6 secretion.[30] The nuclear factor-kappa B signaling pathway, a key regulator of inflammatory responses, may be another mechanism by which FTO modulates IL-6 secretion. Future research should aim to elucidate the molecular pathways through which FTO influences IL-6 production in M2-polarized KCs. Our study uniquely highlights the specific relationship between FTO and IL-6 in KCs, revealing a previously unexplored mechanism by which FTO modulates the immune microenvironment in IBDS.

The findings of this study have important clinical implications for managing IBDS. By identifying FTO as a key regulator of KC polarization and IL-6 secretion, we reveal a potential therapeutic target for disrupting the inflammatory cascade that drives biliary epithelial cell proliferation and disease progression. Targeting FTO could reduce KC M2 polarization and IL-6 production, thereby limiting bile duct strictures and stone formation. Moreover, FTO could serve as a biomarker for IBDS severity, helping identify high-risk patients and guide early intervention. These insights pave the way for future development of FTO inhibitors, which could offer a novel approach to improve IBDS outcomes by addressing the root causes of the disease.

One limitation of our study is that the experiments were primarily conducted *in vitro* and may not fully capture the complexity of the IBDS microenvironment *in vivo*. Although we focused on the JNK/p38 signaling pathway, other pathways may also contribute to the effects of FTO on KC polarization and IL-6 secretion. *In vivo* studies and the investigation of alternative signaling pathways are necessary to comprehensively understand FTO's role in IBDS pathogenesis. Future studies should also investigate the therapeutic potential of FTO-specific inhibitors in IBDS treatment, focusing on their efficacy in regulating KC polarization and reducing IL-6-mediated bile duct stenosis. The safety and specificity of FTO inhibition should be evaluated to assess its clinical feasibility. In conclusion, this study highlights the critical role of FTO in promoting the M2 polarization of KCs and the secretion of IL-6, which drive the pathological proliferation and migration of biliary epithelial cells in IBDS. These findings provide new insights into the molecular mechanisms underlying IBDS progression and suggest that targeting FTO may offer a novel therapeutic approach for managing this disease. By demonstrating the relationship between FTO and IL-6, our study establishes a foundation for future research aimed at exploring FTO as a potential biomarker and therapeutic target in IBDS.

SUMMARY

This study identifies a novel role for the RNA demethylase FTO in the pathogenesis of IBDS through its regulation of KC polarization and IL-6 secretion. We demonstrated that FTO promotes the M2 polarization of KCs and consequently enhances IL-6 secretion, thereby driving the pathological proliferation and migration of biliary epithelial cells. These findings provide significant insights into the molecular mechanisms underlying IBDS progression and suggest that FTO may be a promising therapeutic target. Future clinical investigations and the development of FTO inhibitors could open new avenues for managing IBDS and improving patient outcomes by addressing its root causes.

AVAILABILITY OF DATA AND MATERIALS

The datasets generated and/or analyzed during the present study are available from the corresponding author on reasonable request. All materials, including reagents and protocols, can also be provided on request to ensure reproducibility and facilitate further research.

ABBREVIATIONS

AKT – Protein kinase B
BSA – Bovine serum albumin
DAPI – 4′,6-Diamidino-2-phenylindole
DMSO – Dimethyl sulfoxide
ECL – Enhanced chemiluminescence
EdU – 5-Ethynyl-2'-deoxyuridine
ELISA – Enzyme-linked immunosorbent assay
FTO – Fat mass and obesity-associated protein
GAPDH – Glyceraldehyde-3-phosphate dehydrogenase
HiBEC – Human intrahepatic biliary epithelial cell
HRP – Horseradish peroxidase
IBDS – Intrahepatic bile duct stones
IHC – Immunohistochemistry
IL-6 – Interleukin-6
JNK – c-Jun N-terminal kinase
KCs – Kupffer cells
m6A – N6-methyladenosine
PBS – Phosphate-buffered saline
PET – Polyethylene terephthalate
PI3K – Phosphoinositide 3-kinase
RT-qPCR – Real-time quantitative polymerase chain reaction
SD – Standard deviation
siRNA – Small interfering RNA
STAT3 – Signal transducer and activator of transcription 3
TFA – Trifluoroacetic acid
TNF-α – Tumor necrosis factor-alpha

AUTHOR CONTRIBUTIONS

LXL, QSY, HP, ZYL and FHZ: Contributed to the conceptualization and design of the study; LXL: Conducted the experiments and collected the data; HP and ZYL: Performed data analysis and visualization; FHZ: Provided experimental support and resources; QSY: Supervised the study, acquired funding, and approved the final manuscript. All authors contributed to manuscript preparation and revision and approved the submitted version.

ETHICS APPROVAL AND CONSENT TO PARTICIPATE

The research/study approved by the Institutional Review Board at Medical Ethics Committee of Lujiang People's Hospital, number LYWZLL202304, dated 202304. The authors certify that they have obtained all appropriate patient consent.

ACKNOWLEDGMENTS

The authors would like to express their sincere gratitude to the individuals who provided valuable guidance and technical support during this research. Special thanks go to the team members who contributed to the sample collection and experimental assistance.

FUNDING

Not applicable.

CONFLICT OF INTEREST

The authors declare no conflict of interest.

EDITORIAL/PEER REVIEW

To ensure the integrity and highest quality of CytoJournal publications, the review process of this manuscript was conducted under a **double-blind model** (authors are blinded for reviewers and vice versa) through an automatic online system.

REFERENCES

1. Xia H, Zhang H, Xin X, Liang B, Yang T, Liu Y, *et al*. Surgical management of recurrence of primary intrahepatic bile duct stones. Can J Gastroenterol Hepatol 2023;2023:5158580.
2. Digby KH. Common-duct stones of liver origin. Br J Surg 1930;17:578-91.
3. Yao D, Wu S. Application of laparoscopic technique in the treatment of hepatolithiasis. Surg Laparosc Endosc Percutan Tech 2020;31:247-53.
4. Kim HJ, Kim JS, Joo MK, Lee BJ, Kim JH, Yeon JE, *et al*. Hepatolithiasis and intrahepatic cholangiocarcinoma: A review. World J Gastroenterol 2015;21:13418-31.
5. Yoo ES, Yoo BM, Kim JH, Hwang JC, Yang MJ, Lee KM, *et al*. Evaluation of risk factors for recurrent primary common bile duct stone in patients with cholecystectomy. Scand J Gastroenterol 2018;53:466-70.
6. Motta RV, Saffioti F, Mavroeidis VK. Hepatolithiasis: Epidemiology, presentation, classification and management of a complex disease. World J Gastroenterol 2024;30:1836-50.
7. Lorio E, Patel P, Rosenkranz L, Patel S, Sayana H. Management of hepatolithiasis: Review of the literature. Curr Gastroenterol Rep 2020;22:30.
8. Kim TI, Han SY, Lee J, Kim DU. Removal of intrahepatic bile duct stone could reduce the risk of cholangiocarcinoma: A single-center retrospective study in South Korea. World J Clin Cases 2024;12:913-21.
9. Ran X, Yin B, Ma B. Four major factors contributing to intrahepatic stones. Gastroenterol Res Pract 2017;2017:7213043.

10. Lazaridis KN, LaRusso NF. The cholangiopathies. Mayo Clin Proc 2015;90:791-800.
11. Nejak-Bowen K. If it looks like a duct and acts like a duct: On the role of reprogrammed hepatocytes in cholangiopathies. Gene Expr 2020;20:19-23.
12. Bennett H, Troutman TD, Sakai M, Glass CK. Epigenetic regulation of Kupffer cell function in health and disease. Front Immunol 2020;11:609618.
13. Lee JL, Wang YC, Hsu YA, Chen CS, Weng RC, Lu YP, *et al*. Galectin-12 modulates Kupffer cell polarization to alter the progression of nonalcoholic fatty liver disease. Glycobiology 2023;33:673-82.
14. Ding X, Pang Y, Liu Q, Zhang H, Wu J, Lei J, *et al*. GO-PEG represses the progression of liver inflammation via regulating the M1/M2 polarization of Kupffer cells. Small 2024;20:e2306483.
15. Luo W, Xu Q, Wang Q, Wu H, Hua J. Effect of modulation of PPAR-γ activity on Kupffer cells M_1/M_2 polarization in the development of non-alcoholic fatty liver disease. Sci Rep 2017;7:44612.
16. Flores Molina M, Abdelnabi MN, Mazouz S, Villafranca-Baughman D, Trinh VQ, Muhammad S, *et al*. Distinct spatial distribution and roles of Kupffer cells and monocyte-derived macrophages in mouse acute liver injury. Front Immunol 2022;13:994480.
17. Jordan SC, Choi J, Kim I, Wu G, Toyoda M, Shin B, *et al*. Interleukin-6, A cytokine critical to mediation of inflammation, autoimmunity and allograft rejection: Therapeutic implications of IL-6 receptor blockade. Transplantation 2017;101:32-44.
18. Jeffery HC, Hunter S, Humphreys EH, Bhogal R, Wawman RE, Birtwistle J, *et al*. Bidirectional cross-talk between biliary epithelium and Th17 cells promotes local Th17 expansion and bile duct proliferation in biliary liver diseases. J Immunol 2019;203:1151-9.
19. Sato K, Hall C, Glaser S, Francis H, Meng F, Alpini G. Pathogenesis of Kupffer cells in cholestatic liver injury. Am J Pathol 2016;186:2238-47.
20. Wang C, Ma C, Gong L, Guo Y, Fu K, Zhang Y, *et al*. Macrophage polarization and its role in liver disease. Front Immunol 2021;12:803037.
21. Zhou Y, Chen S, Yang F, Zhang Y, Xiong L, Zhao J, *et al*. Rabeprazole suppresses cell proliferation in gastric epithelial cells by targeting $STAT_3$-mediated glycolysis. Biochem Pharmacol 2021;188:114525.
22. Chen CH, Lin CL, Kao CH. Association between inflammatory bowel disease and cholelithiasis: A nationwide population-based cohort study. Int J Environ Res Public Health 2018;15:513.
23. Hyun JJ, Irani SS, Ross AS, Larsen MC, Gluck M, Kozarek RA. Incidence and significance of biliary stricture in chronic pancreatitis patients undergoing extracorporeal shock wave lithotripsy for obstructing pancreatic duct stones. Gut Liver 2021;15:128-34.
24. Ozcan N, Riaz A, Kahriman G. Percutaneous management of biliary stones. Semin Intervent Radiol 2021;38:348-55.
25. Licá IC, Frazão GC, Nogueira RA, Lira MG, Dos Santos VA, Rodrigues JG, *et al*. Immunological mechanisms involved in macrophage activation and polarization in schistosomiasis. Parasitology 2023;150:401-15.
26. Gan X, Dai Z, Ge C, Yin H, Wang Y, Tan J, *et al*. FTO promotes liver inflammation by suppressing m6A mRNA methylation of IL-17RA. Front Oncol 2022;12:989353.
27. Zahr T, Sun K, Qiang L. The polarizable and reprogrammable identity of Kupffer cells in nonalcoholic steatohepatitis. Med Rev (2021) 2022;2:324-7.
28. Chen B, Chen Q, Lu M, Zou E, Lin G, Yao J, *et al*. Hypocrellin A against intrahepatic cholangiocarcinoma via multi-target inhibition of the PI3K-AKT-mTOR, MAPK, and STAT3 signaling pathways. Phytomedicine 2024;135:156022.
29. Zeng B, Wu R, Chen Y, Chen W, Liu Y, Liao X, *et al*. FTO knockout in adipose tissue effectively alleviates hepatic steatosis partially via increasing the secretion of adipocyte-derived IL-6. Gene 2022;818:146224.
30. Izquierdo V, Palomera-Ávalos V, Pallàs M, Griñán-Ferré C. Resveratrol supplementation attenuates cognitive and molecular alterations under maternal high-fat diet intake: Epigenetic inheritance over generations. Int J Mol Sci 2021;22:1453.

How to cite this article: Li L, Peng H, Li Z, Zhou F, Yu Q. FTO-mediated regulation of Kupffer cell polarization and interleukin-6 secretion promotes biliary epithelial cell proliferation in intrahepatic bile duct stones. CytoJournal. 2024;21:83. doi: 10.25259/Cytojournal_193_2024

HTML of this article is available FREE at:
https://dx.doi.org/10.25259/Cytojournal_193_2024